



Late Quaternary (Holocene) landscape evolution of a monsoon-influenced high Himalayan valley, Gori Ganga, Nanda Devi, NE Garhwal

Patrick L. Barnard^{a,b}, Lewis A. Owen^{a,*}, Milap C. Sharma^c, Robert C. Finkel^{a,b}

^aDepartment of Earth Sciences, University of California, Riverside, CA 92521-0423, USA

^bCenter for Accelerator Mass Spectrometry, Lawrence Livermore National Laboratory, Livermore, CA 94550, USA

^cCentre for the study of Regional Development, Jawaharlal Nehru University, New Delhi 110 067, India

Received 16 April 2003; received in revised form 8 September 2003; accepted 1 December 2003

Available online 25 January 2004

Abstract

The Garhwal Himalaya provides an excellent natural laboratory in which to examine landscape evolution in a monsoon-influenced high mountain environment. Geomorphic and sedimentological analysis and ¹⁰Be cosmogenic radionuclide (CRN) surface exposure dating of moraines, fans, and river and strath terraces in the Gori Ganga Valley of Nanda Devi, NE Garhwal, indicate that fans and river terraces developed rapidly by debris flow and flood processes during periods of deglaciation. These phases of high sediment transfer occurred at ~ 1–2, ~ 4–5, and ~ 7–8 ka. Fan incision rates, subsequent to major times of resedimentation after each glacial advance, are between ~ 19 and 57 mm/year. This contrasts with bedrock incision rates, based on mid-Holocene strath terraces, of ~ 5 mm/year. These rates indicate that despite episodes of rapid denudation and resedimentation linked to glacial activity in this region, the background rates of denudation are similar to those for other regions of the Himalaya, averaging several millimeters per year. Furthermore, these data show the importance of climatic controls on landscape evolution and suggest a strong monsoonal control on the dynamics of earth surface processes in this region.

© 2003 Elsevier B.V. All rights reserved.

Keywords: Garhwal Himalaya; Quaternary; Terrace and fan development; Denudation rates; Glaciation

1. Introduction

The dynamics and rates of landscape evolution in glaciated Himalayan environments are poorly understood. This is especially the case in monsoon-influenced regions where access is particularly difficult.

To help elucidate the origins of landforms and to quantify rates of landscape evolution in such an environment, we undertook a study of the upper Gori Ganga drainage basin in the Nanda Devi region of NE Garhwal (Kumaun) Himalaya (Fig. 1). More specifically, we examine the relationship between glaciation and debris flow fan development to test the hypothesis that landscape evolution, in particular sediment transfer, is most intense over short intervals of time during periods of deglaciation.

* Corresponding author. Tel.: +1-909-787-3106; fax: +1-909-787-3106.

E-mail address: lewis.owen@ucr.edu (L.A. Owen).

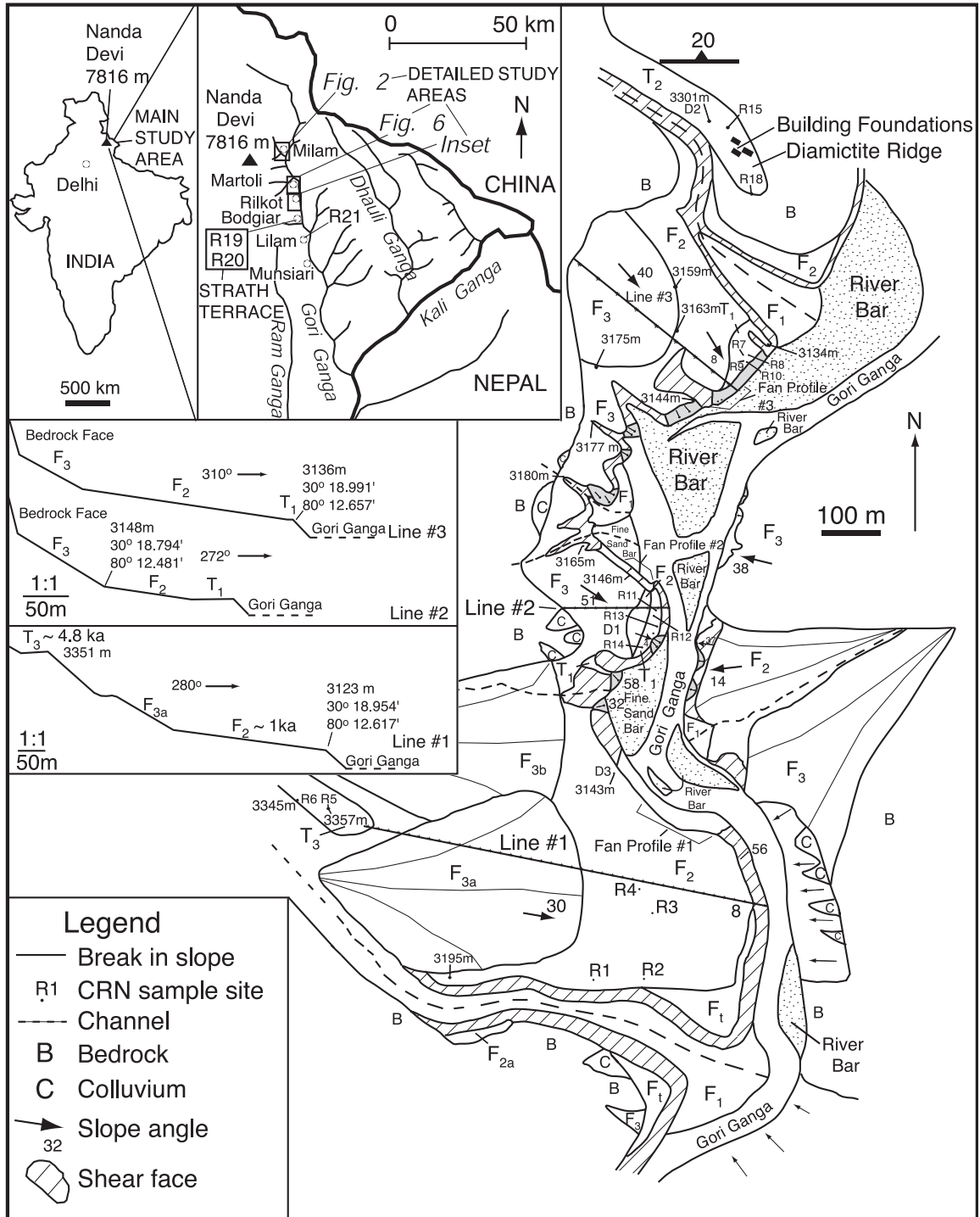


Fig. 1. Gori Ganga study area with Rilkot geomorphic map and cross-sectional profiles. The following datum points are included in the map: D1 = 30° 18.762' N, 80° 12.549' E, 3140 m; D2 = 30° 19.209' N, 80° 12.620' E, 3301 m; D3 = 30° 18.638' N, 80° 12.511' E, 3143 m.

With the exception of two minor studies (Janapangi, 1975; Kumar et al., 1975), no prior geomorphic research has been conducted in the Gori Ganga Valley. In the valleys to the west of the Gori Ganga region in western Garhwal, however, several studies have examined the style of landscape evolution (Owen et al., 1995, 1996; Sharma and Owen, 1996; Owen and Sharma, 1998; Barnard et al., 2001, in press). These studies showed that the monsoon is probably the dominant forcing factor on natural denudation and landscape evolution in these high mountains. Our work in the NE Garhwal Himalaya was designed to test this conclusion by examining a similar setting to the immediate east. We concentrated on examining the nature and timing of fan sedimentation in the upper Gori Ganga catchment, and calculating rates of bedrock and fan incision to aid in understanding the dynamics, magnitude, and frequency of earth surface processes in the landscape evolution of a monsoon-influenced continental–continental collision zone.

2. Research area

The Gori Ganga Valley is situated between Tibet and Nepal on the eastern slope of Nanda Devi in NE Garhwal Himalaya of northern India (Fig. 1). The primary study area is located ~ 500 km NE of New Delhi and extends north from the town of Rilkot (3143 m asl) to Milam village (3423 m asl) and the snout of the Milam Glacier (3536 m asl), a total distance of 12 km. Strath terraces were also studied south of Rilkot at Bogdiar (2315 m asl) and Lilam (1412 m asl; Fig. 1).

The Gori Ganga (Ganga = river) drainage basin is an important source for the Ganges River. The Gori Ganga originates in glaciated mountains of the NE Garhwal Himalaya that contain peaks that exceed 7000 m asl, the highest being Nanda Devi at 7816 m asl. Nanda Devi is the highest mountain in the central Himalaya and the highest mountain contained solely within India (Heim and Gansser, 1975). A substantial component of the Gori Ganga drainage comes from the Milam Glacier, although the hydrological characteristics of the Gori Ganga have yet to be quantified. The SW Asian summer monsoon provides most of the annual precipitation of 1550 mm between June and August (Indian Meteorological Department, 1989).

Bojar et al. (2001) undertook a structural analysis along the Gori Ganga Valley between Martoli and Munsyari and identified four distinct structural terrains. These terrains are described by Valdiya (1980) and Paul (1998) and include, from north to south in the Gori Ganga Valley: (i) Tethyan Zone; (ii) High Himalayan Crystalline; (iii) Lesser Himalayan Crystalline; and (iv) Lesser Himalayan Krol Nappe. Three major suture zones separate these zones from each other: South Tibetan Detachment Zone, Main Central Thrust Zone, and Munsyari Thrust, respectively. The bedrock consists mostly of low- to medium-grade slate, phyllite, quartzite, and schist. Higher-grade, garnet-bearing schists and granogneissic rocks are present south of Rilkot. Slates, phyllites, and schists within the study area have well-developed foliation with cleavage planes striking almost due west and dipping 20° N. Diamicrites also occur within the study area, outcropping in a pronounced ridge that trends east, normal to the flow of the Gori Ganga (Fig. 1).

Large landslides (>1000 m³) are common within the region and are dominantly controlled by foliation in the metamorphic rocks. Several of these landslides incorporate several million cubic meters of debris and are intensely eroded. Smaller-scale slope failures are common within the contemporary riverbank. Paul et al. (2000) described a recent large-scale mass movement (>1 million m³) in the Kali Ganga Valley (see Fig. 1) of Kumaun Himalaya, 50 km SE of Rilkot. They showed that most major landslides, including complex debris flow-rock falls, occur during the monsoon season, sometimes completely or partially blocking the drainage. Weidinger (1998) studied modern lake-damming landslides in the Birahi Ganga Valley west of the Gori Ganga Valley and in western Nepal. Weidinger (1998) discussed the importance of tectonic, lithological, morphological, and climatic conditions for triggering landslides in the Himalaya and showed the immediate high risk of flooding downvalley if landslide-produced dams break catastrophically. The geomorphic consequences of dam breaking are massive erosion, sediment transport, and the formation of flood terraces downvalley.

Numerous channel bars are present throughout the upper Gori Ganga Valley, consisting mostly of cobbles, sand, and silt, mainly of glacial origin. Channel

bars are densely concentrated behind debris fans that have recently blocked the Gori Ganga.

South of Rilkot, the river gradient increases and the channel becomes confined within a narrow gorge (Fig. 1). The abrupt change in gradient is most likely due to a shift from a glaciated to nonglaciated valley morphology, as well as a change in rock type from low- and medium-grade metamorphic rocks north of Rilkot, to medium- and high-grade metamorphic rocks to the south of Rilkot.

3. Methods

3.1. Field methods

Two main study areas were chosen to examine the relationship between glaciation and fan development: one adjacent to the Milam Glacier and the other downvalley at the former terminus of the glacier at Rilkot (Fig. 1). In the Milam Glacier field area, detailed geomorphic mapping was undertaken and samples for CRN dating were collected from moraines and fans to develop a glacial chronology and to examine the formation of the moraines with adjacent fans and terraces. The study area at Rilkot contained a well-preserved set of fans and terraces (Fig. 1). Geomorphic maps were constructed, fans were sampled for CRN dating, and graphic sedimentary logs were made of selected sections within the fans. Each

map was constructed using a handheld global positioning system (GPS), rangefinder, and compass. Three strath terraces were sampled downvalley of Rilkot (two at Bogdiar, one at Lilam: Fig. 1) to determine the timing of strath formation and to calculate bedrock incision rates for the region.

Samples for CRN dating were collected from the tops of meter-sized boulders by chiseling off a 1-cm-thick horizontal surface layer. Boulders were selected that were partially buried but had at least 1 m of relief and were located along the distal edges of fan surfaces or along moraine ridges. These specifications reduced the likelihood that a boulder had toppled or been exhumed. Multiple samples were taken from each landform to provide confidence in the reproducibility of the dating and to estimate CRN inheritance. Weathering, inheritance, and other effects produce scatter in CRN concentrations from different boulders on the same landform. For erosion rates of $1\text{--}5\text{ m Ma}^{-1}$ on surface boulders, an exposure age of 10 ka would underestimate the true age by 1–4% (Owen et al., 2002; Finkel et al., 2003). Denudation rates were calculated using the CRN ages and cross-valley profiles that were surveyed across the fan surfaces down to the present level of the Gori Ganga.

3.2. Laboratory analysis

CRN samples were processed at Lawrence Livermore National Laboratory by measuring ^{10}Be

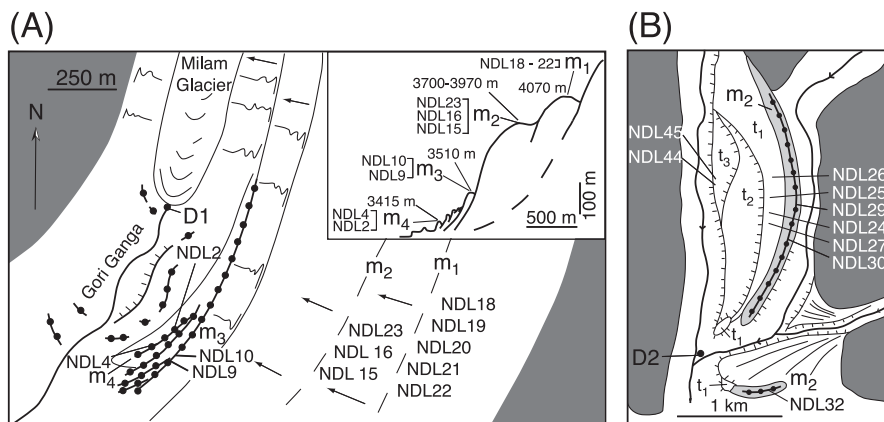


Fig. 2. Moraines and terraces in the upper Gori Ganga Valley. (A) Geomorphic map and profile in the vicinity of the Milam Glacier. (B) Geomorphic map in the vicinity of Milam village. The following datum points are included in the map: D1 = $30^{\circ} 27.783' \text{ N.}, 80^{\circ} 07.751' \text{ E.}, 3532 \text{ m}$; D2 = $30^{\circ} 24.849' \text{ N.}, 80^{\circ} 09.467' \text{ E.}, 3350 \text{ m}$.

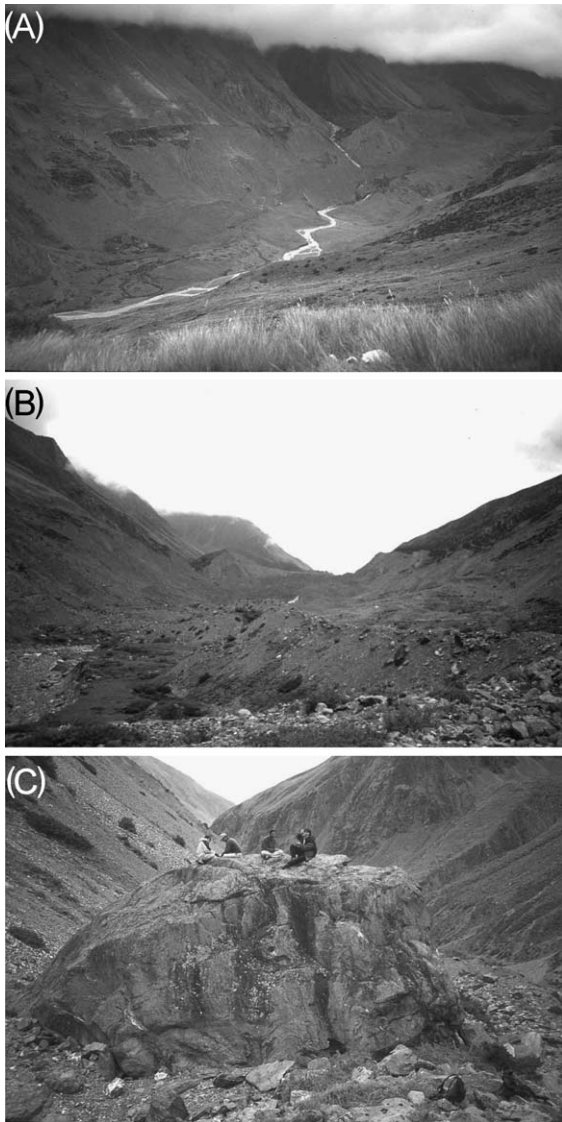


Fig. 3. Latero-frontal moraines adjacent to the Milam glacier. (A) View looking north at the snout of the Milam glacier showing the Holocene moraines. (B) View looking north at a Little Ice Age moraine. (C) View of a typical sampling site for CRN dating on a Holocene moraine. Sample site for NDL9 is pictured.

($t_{1/2} = 1.5 \times 10^6$ year) in quartz (Kohl and Nishiizumi, 1992). Each rock sample was crushed and sieved, and the quartz was isolated by leaching 100 g of the 250–500 μm fraction in a series of HCl and HF/HNO₃ baths (for methodology, see Kohl and Nishiizumi, 1992). Be carrier was added to the cleaned quartz,

and the sample was then dissolved in 3:1 HF/HNO₃ to dissolve the quartz and release ¹⁰Be from the crystal structure. Be was purified using ion exchange chromatography and precipitation and then ignited in a furnace to produce BeO. The processed samples were mixed with Nb and loaded into cathodes for determination of ¹⁰Be/⁹Be ratios by accelerator mass spectrometry using the LLNL accelerator mass spec-

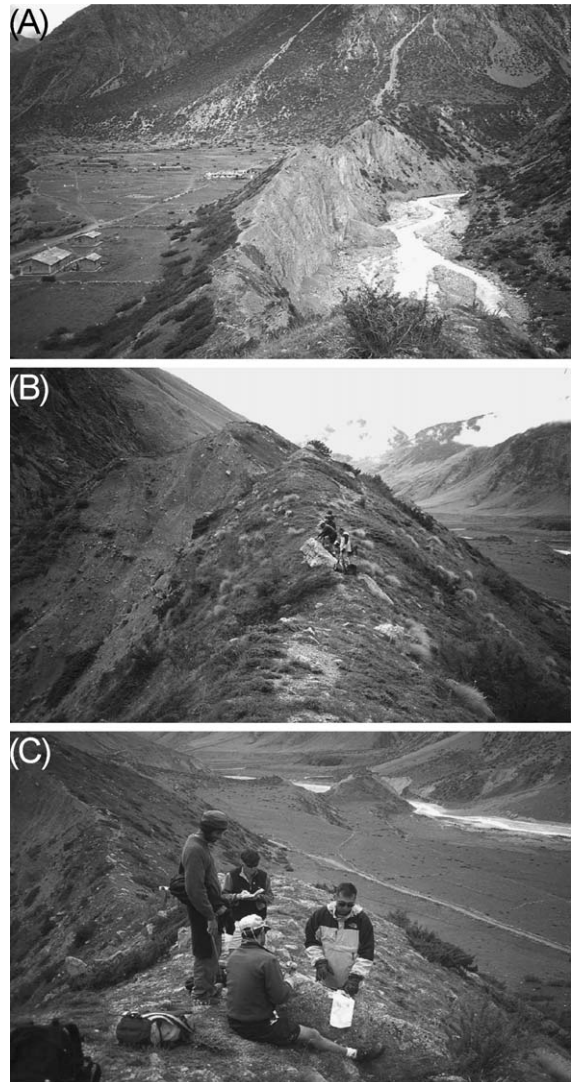


Fig. 4. View of latero-frontal moraine south of Milam village. (A) View looking at the latero-frontal moraines and terraces. (B) View of the moraine crest showing typical sampling locations for CRN dating. Sample site for NDL30 is pictured. (C) View of the moraine crest showing sample site for NDL29.

trometer (Davis et al., 1990). $^{10}\text{Be}/^9\text{Be}$ ratios were determined relative to an ICN ^{10}Be standard prepared by K. Nishiizumi using a half-life of 1.5×10^6 years. Age determinations were based on the equations and production rates in Lal (1991) as modified by Stone (2000). A correction for variation in the geomagnetic field was applied to determine the final age of each sample as described in Nishiizumi et al. (1989) using the SINT800 geomagnetic intensity assessment (J.-P. Valet, University of Paris-VII, Institut de Physique du Globe de Paris, personal communication, 1990) Full details of the methodology used in the age determination are described in Owen et al. (2001, 2002).

4. Moraine geomorphology and CRN sampling sites

Five main sets of nested moraine ridges are adjacent to the Milam Glacier (Fig. 2). From young-

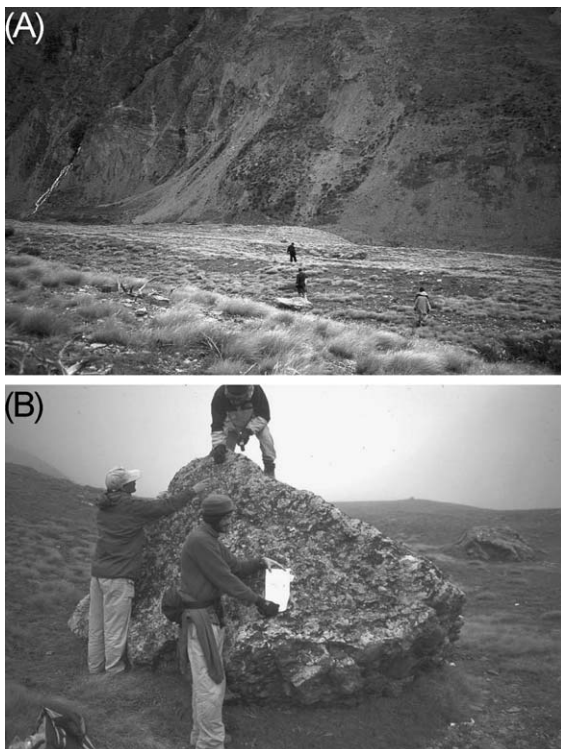


Fig. 5. Views of high moraines above the Milam glacier. (A) Subdued moraines at an altitude of 3900 m asl. (B) Boulder sampled for NDL16 on the highest and oldest moraine ridge at ~ 4100 m asl.

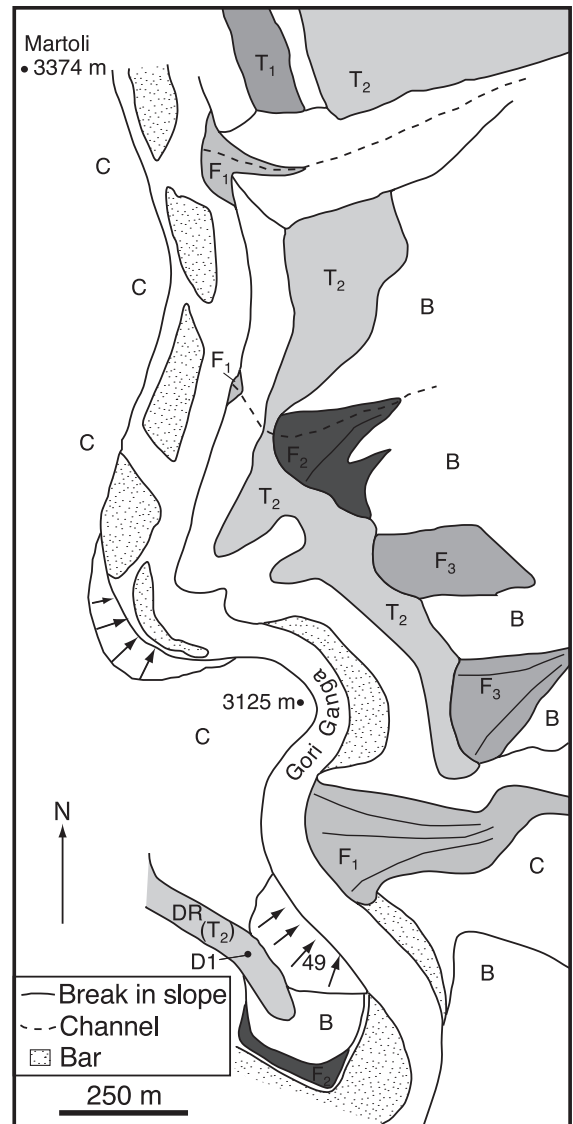


Fig. 6. Geomorphic map of the area north of Rilkot (B=bedrock, C=colluvium, DR=diamictite ridge). The following datum point is mapped: D2 = $30^{\circ} 19.209' \text{ N.}$, $80^{\circ} 12.620' \text{ E.}$, 3301 m.

gest to oldest, these moraines rise in elevation from the valley floor at ~ 3500 to ~ 4100 m asl. The youngest three sets of latero-frontal moraines are sharp crested and are composed of angular boulders that are not weathered. Subsidiary ridges are present on each of these moraines (Fig. 2). Samples NDL2, NDL4, NDL9, and NDL10 were collected from boulders on the crests of two of these moraines

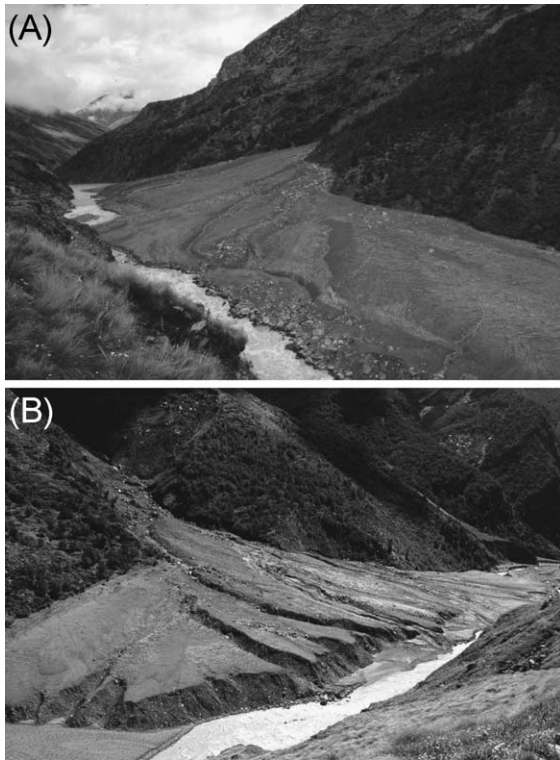


Fig. 7. Recent fan development below Rilkot that may have restricted channel flow and reduced the gradient of the Gori Ganga. (A) View upvalley of fan. (B) Crossvalley view of fan. Note cut bank erosion by Gori Ganga.

(Figs. 2A and 3). A well-vegetated, subdued, and eroded lateral moraine is present above the fresh young moraines at an altitude of between 3700 and 3970 m asl (Figs. 2A and 3A). This moraine can be traced for several kilometers upvalley from the snout of the Milam Glacier (Fig. 2A). The moraine is discontinuous below the Milam Glacier, but forms an impressive latero-frontal moraine near Milam village (Fig. 4). Samples NDL15, NDL16, and NDL23 were collected from boulders that were on top of small subdued ridges of this moraine above Milam Glacier and samples NDL29 and NDL30 were collected from the crest of the latero-frontal moraine at Milam village (Fig. 4). A small moraine ridge south of the latero-frontal moraine might represent an earlier stage of the glacial advance that produced the main latero-frontal moraine at Milam. Sample NDL32 was collected from a boulder on the crest of this moraine. The highest moraine comprises

irregular, valley-parallel, subdued, and well-vegetated ridges that form a relatively broad bench along the valley at an altitude of between 4000 and 4100 m asl (Fig. 5A). Samples NDL18 to NDL22 were collected from boulders on the crests of these ridges. The boulders that were sampled were >2 m in diameter (Fig. 5B).

No equivalent age moraines are present down-valley of Milam. A moraine fragment is found along the eastside of the valley between Milam and Rilkot but was not included in our study. Samples R15 and R18 were collected along the crest of a diamictite ridge above Rilkot (Figs. 1 and 6).

5. Fan geomorphology and sedimentology

On the basis of geomorphology, three types of fans are present in the Rilkot area. These are designated as

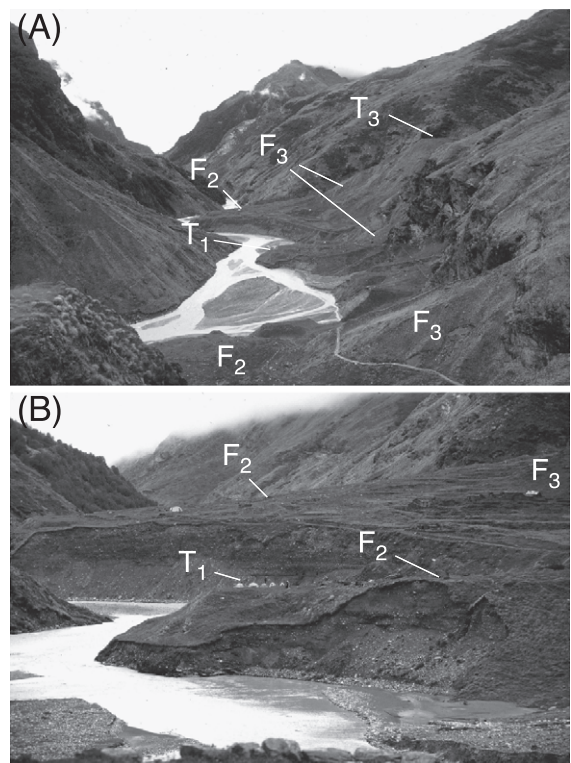


Fig. 8. Views from the diamictite ridge south toward Rilkot and the fans and terraces mapped in Fig. 1. (A) Overview. (B) Enlarged view illustrating the close morphostratigraphic relationship between F_3 , F_2 , and T_1 .



Fig. 9. View looking down, in an easterly direction, on the southernmost F_2 fan at Rilkot from the surface of T_3 (see Fig. 1). Note the progressive incision of the F_2 fan by F_t and F_1 .

F_1 , F_2 , and F_3 on the geomorphic maps and plates (Figs. 1, 6 and 10). F_1 and F_2 are analogous to Owen's (1989) description of debris terraces in the Karakoram

Mountains of northern Pakistan. F_3 deposits are similar to Owen's (1989) description of high-angle scree fans. In addition, one intermediate and incised fan feature between F_1 and F_2 is present and is referred to as a debris fan terrace F_t . The geomorphic maps show that the fan surfaces slope down from the side valleys toward the main valley (Figs. 1 and 6).

The F_1 fans are actively aggrading into the main river channel. These fans contain stream channels that drain side canyons and the mountains surrounding the Gori Ganga Valley and often incise terraces in the older host fans. Lobes of F_1 fans commonly extend into the river and narrow the channel width (Figs. 6 and 7). The 20-m-high cut banks in fresh, unvegetated debris fan material suggest that the Gori Ganga was at least partially blocked during periods of rapid debris aggradation. The debris fans height and slope easily project across the Gori

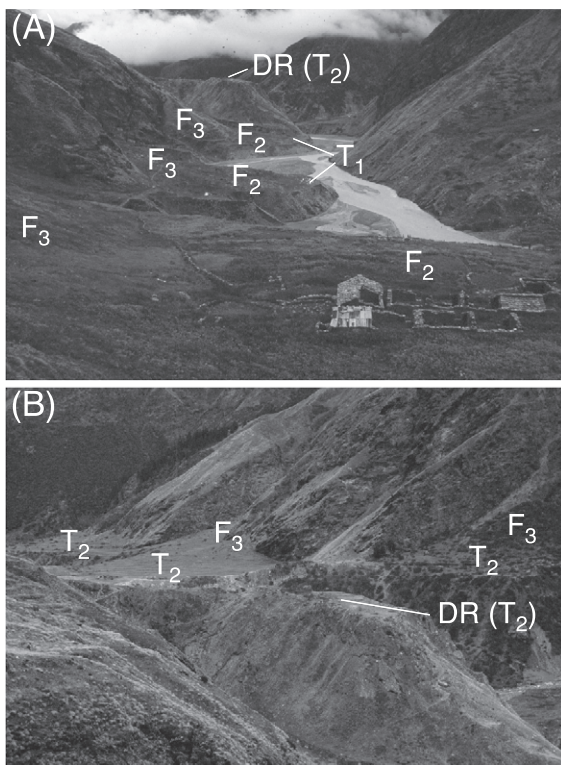


Fig. 10. Views north of the diamictite ridge (DR) from the top of T_3 . (A) View from Rilkot (foreground) showing fans and terraces mapped in Fig. 1. (B) Diamictite ridge with equivalent terraces (T_2) and fans on the opposite side of the valley.

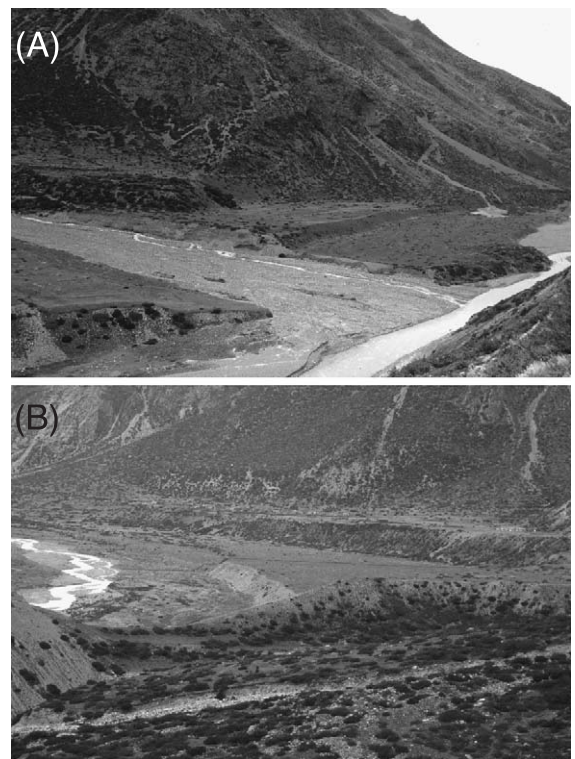


Fig. 11. Terraces in the Milam area. (A) Terrace succession on the west side of the Gori Ganga 2 km south of Milam. (B) Terrace succession at Milam. The village is situated on the highest terrace (upper right).

Ganga providing further evidence of prior blockage. Owen (1989) and Weidinger (1998) described events where large lakes have been impounded behind fans in the Himalaya. The effects of damming by F_1 fans are recorded in the sedimentary record of the study area by fine sediment bars that accumulate directly behind large F_1 fans that built out into the river channel.

F_2 fans ($\sim 8^\circ$) occur up the valley sides, are usually incised by F_1 fans (Figs. 8–10), and commonly build out onto inactive terraces. The toes of the F_2 fans are usually truncated by the river or slope failures. F_2 deposits are only slightly incised ($\sim 1\text{--}2$ m deep) by the terraces that they often border.

F_t terraces are commonly situated at an intermediate level between lower F_1 fans and F_2 fans. The F_t deposits are no longer active and are situated

slightly above the F_1 fans that have incised them (Fig. 9).

F_3 fans ($\sim 30\text{--}50^\circ$) are found with the toe of the fan overlapping inactive terraces, interfingered with F_2 fans, or directly at the edge of the main river channel (Figs. 8 and 10). Large boulders (up to 6 m in diameter) are scattered across the surfaces of the F_3 fans. Average clasts are larger in size and have greater angularity than other fans in the study area. Fresh, unweathered exposures in cliffs above the F_3 fans suggest that some boulders within the fan surface below may be the result of recent rock avalanches and rockfalls. F_3 fans represent debris accumulated as talus or scree from small rock avalanches. Both the F_2 and F_3 fans are fully vegetated and are inactive.

The T_1 and T_2 terraces are present throughout the study area (Figs. 8 and 10). They are characterized by their gentle slopes ($0\text{--}4^\circ$) and planar

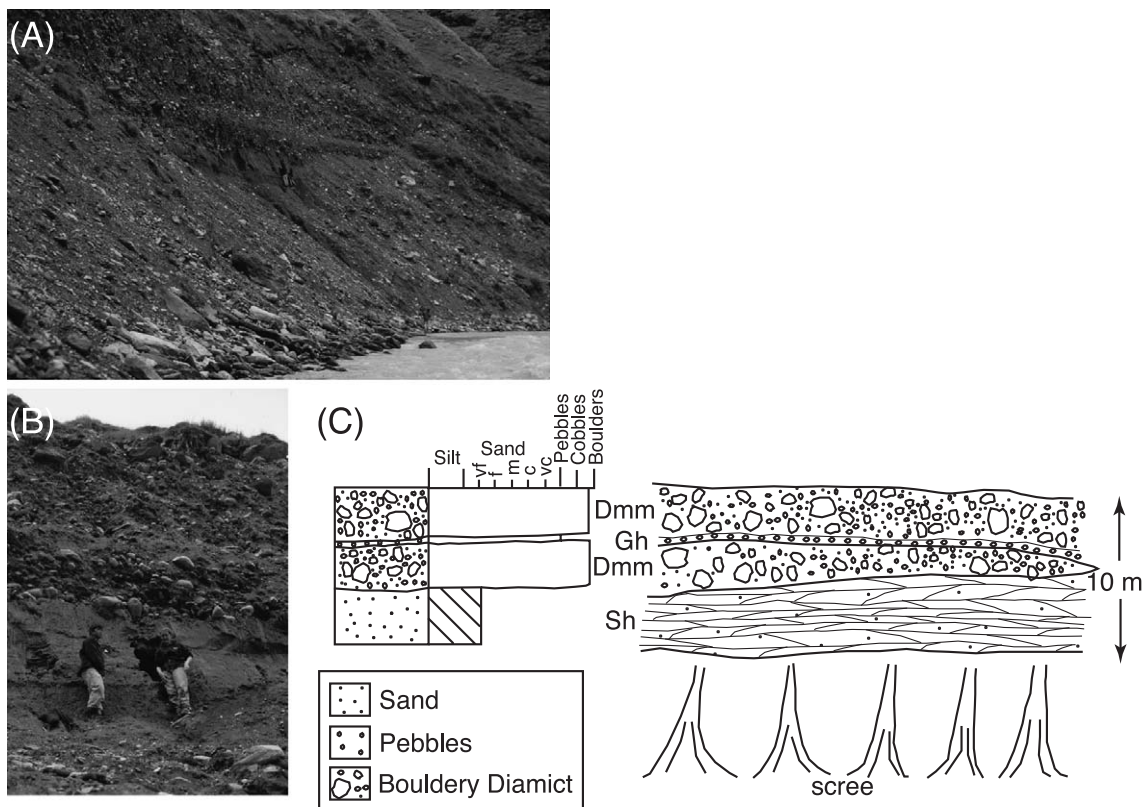


Fig. 12. Southern portion of fan profile #1. (A) View looking north along the section. Note people for scale (center). (B) Close-up of cross-bedded sands at bottom of exposure. (C) Graphic sedimentary log and field sketch. Lithofacies codes after Eyles et al. (1983) as modified by Benn and Evans (1998).

surfaces. These terraces are always found between fan deposits and riverbank slopes. They are located upriver from the fans that in the past may have blocked the Gori Ganga (e.g., the southern most F_2 fan and the diamictite ridge: Fig. 1). These landforms are similar to Owen's (1989) description of lacustrine terraces in the Karakoram Mountains. The geomorphic relationship of the T_1 terraces to the valley morphology suggests that they were constructed during an aggradational period as a result of fans damming the Gori Ganga. Morphostratigraphic evidence suggests that F_2 fans and T_1 terraces correlate with the F_3 fans.

The diamictite ridge above Rilkot (Figs. 1, 6, 8 and 10) is identified as T_2 because it is at the same stratigraphic level as T_2 -designated terraces across the valley. Sections in the ridge contain moderately lithified deposits of poorly sorted boulders and cobbles with an isotropic clast fabric, supported in a matrix of silt and clay. The surface of the flat-topped ridge has an elevation of 3301 m asl that is 50 m lower

than feature T_3 . The landform has clearly been reworked by fluvial activity, having created a stream-lined form. The other surfaces designated as T_2 (Figs. 6 and 10B) are much broader, shaped more like classic fluvial terraces.

The T_3 terrace is the highest geomorphic surface mapped in the Rilkot area (Fig. 8A). This stream-lined landform has a pronounced horizontal surface, ~ 50 m wide and 150 m long, and is thickly vegetated with only a few boulders exposed on the surface. It formed within the irregular body of a large landslide complex, but its morphology suggests that it is a fluvial terrace. Based on this conclusion, subsequent landslide failure would have occurred only as erosion slowly lowered the river gradient and would be primarily in the form of debris flows, as is evident from the large F_2 fan built out from the south side of this terrace.

Several terraces were identified in the Milam area, ~ 2 km downvalley from the Milam glacier (Fig. 11). Each of these is extensive (up to 500 m

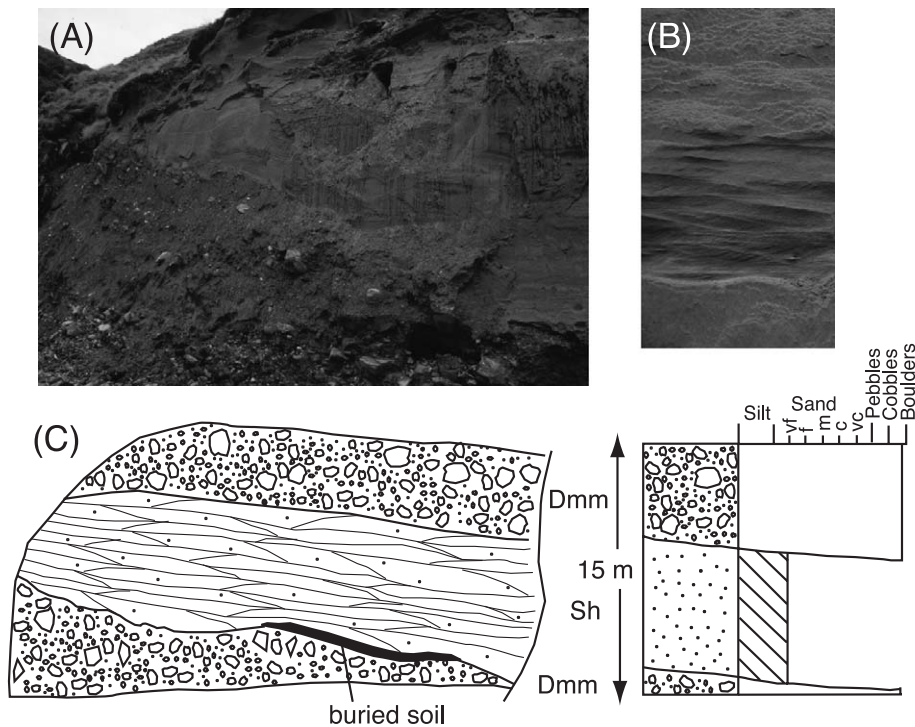


Fig. 13. Section from the northern portion of fan profile #1 near Rilkot. (A) View of the lower half of the exposed fan section showing the contact between the lower diamict unit and sandy unit. (B) Close-up of cross-bedding in very fine sands. (C) Field sketch and graphic sedimentary log of section. Lithofacies codes after Eyles et al. (1983) as modified by Benn and Evans (1998).

wide) and slopes gently ($<4^\circ$) downvalley. Within each succession, the lower terrace steps down toward the valley bottom. Meter-sized, sub-rounded quartzite boulders are scattered on the surfaces.

Each fan that was studied is capped with a diamict unit at least 3 m thick that consists of poorly sorted, massively bedded, subrounded to subangular cobbles

and boulders, supported by a sandy mud matrix. The clasts are often striated and edge-rounded and are occasionally imbricated, but generally have no preferred orientation. The diamicts commonly overlie thinly bedded sands. The three fans sections logged are shown in Figs. 12–14. For location of the profiles, see Fig. 1.

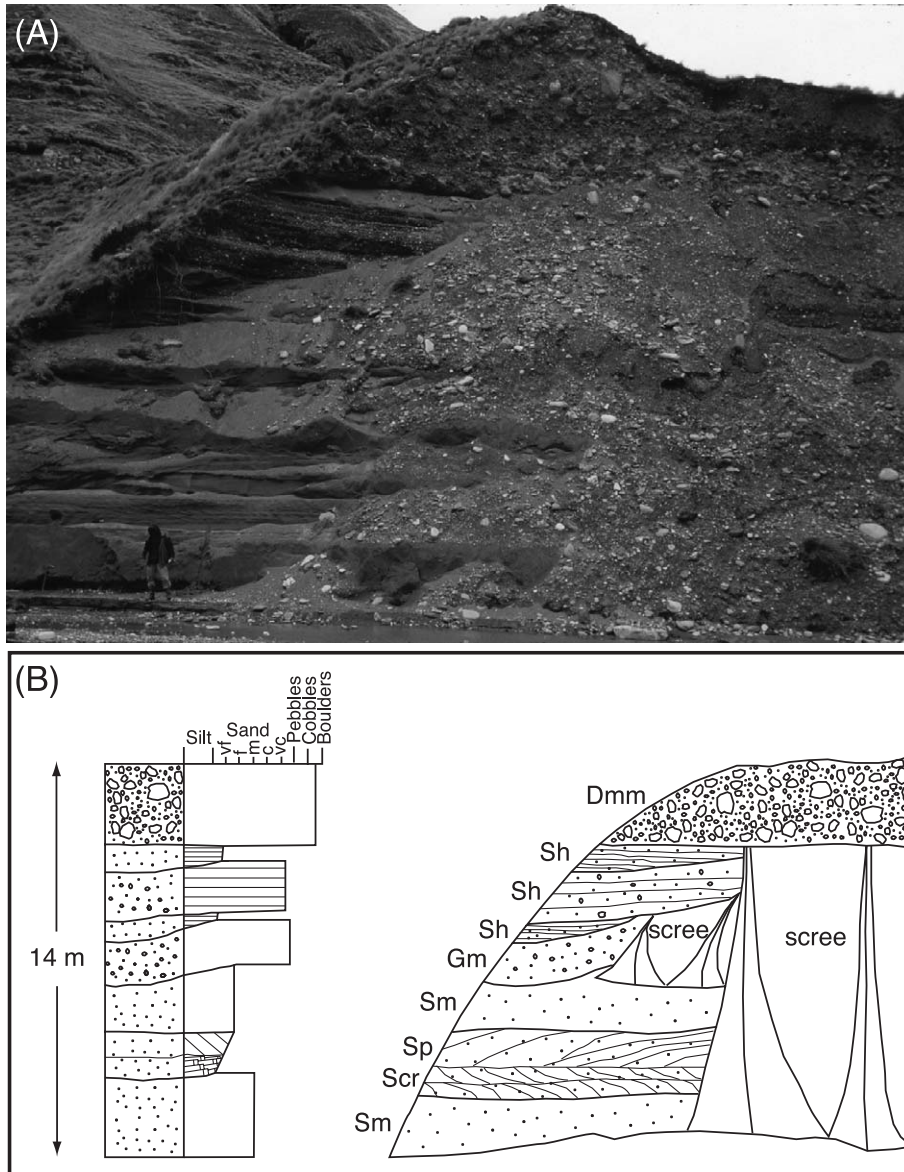


Fig. 14. Fan profile #3. (A) View of entire section. (B) Sedimentary log and sketch showing multiple sandy pebble and pebbly sand units overlain by a 4-m-thick bouldery diamict. Lithofacies codes after Eyles et al. (1983) as modified by Benn and Evans (1998).

The top section on the southern end of profile #1 consists of two 3-m-thick diamict units, separated by a thin, well-sorted, subrounded pebble layer (Fig. 12). The lower diamict unit overlies a 2.5-m-thick unit of thinly bedded (few centimeters), well-sorted fine sands with extensive cross-bedding. The beds in the finer-grained units dip parallel to the gradient of the present fluvial system.

The northern end of fan profile #1 comprises a 5-m-thick, massive, subrounded diamict unit that overlies cross-bedded, very fine sands that overlie a subangular diamict unit (Fig. 13). At the top of the lower diamict unit is a thin layer of organic matter, consisting of grasses with a few woody particles. Involutions and slumped bedding have been found in the sandy layer. Clasts in the diamict units consist of schist and gneiss and measure up to 1.5 m in diameter.

A small exposure in fan profile #2 consists of an upper unit of matrix-supported, bouldery diamict, with an isotropic clast fabric. Scree obscures all but the upper 2 m of the section. Fan profile #3 (Fig. 14) contains the typical subrounded diamict unit on top but overlies at least eight major units of sand and sandy pebble units of varying grain sizes and degrees of cross-bedding, sorting, and bed thickness (a few centimeters to a few tens of centimeters).

6. Strath terraces

Samples R19 and R20 were collected from narrow strath terraces comprising gneissic bedrock in the Gori Ganga gorge near Bogdiar at an altitude of ~ 2300 m (Figs. 1 and 15). Sample R21 was collected from gneissic bedrock much farther down the valley near the village of Lilam (Figs. 1 and 15), at an altitude of 1412 m. These are the only three locations where strath terraces have been identified in the upper Gori Ganga Valley. CRN dating shows that they formed during the mid-Holocene (range from 4.8 to 5.7 ka; Table 1).

7. Moraine succession

The youngest moraines have CRN ages that range from ~ 600 to 140 year (Table 1, Fig. 16). These

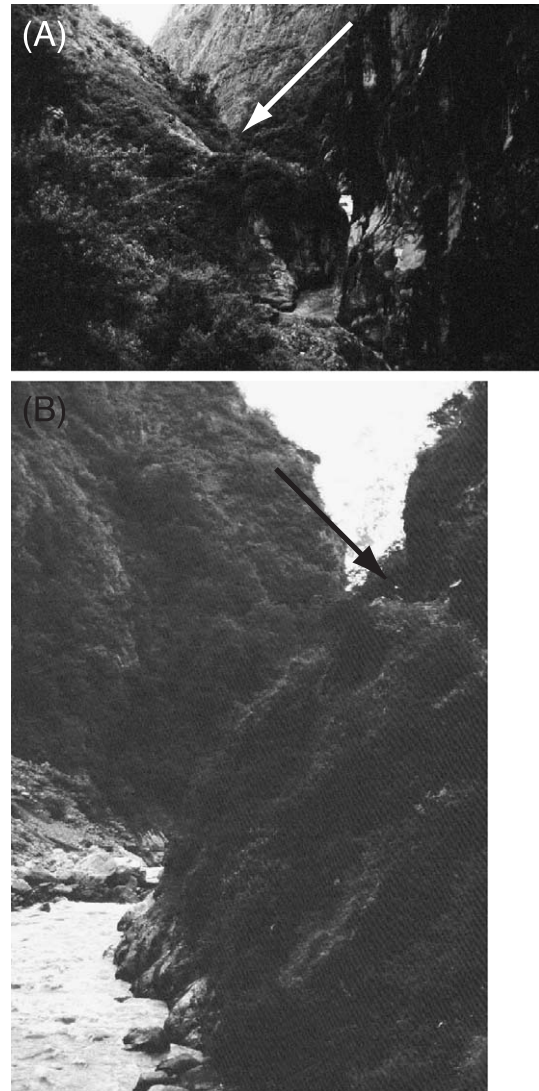


Fig. 15. Strath terraces sampled in the Gori Ganga Valley. (A) View looking north of Bogdiar strath #1 (R19), 26 m above the Gori Ganga. (B) View looking south of Bogdiar strath #2, with the Gori Ganga 32 m below.

moraines probably represent a Little Ice Age (LIA) advance. The latero-frontal moraine at Milam lies at an altitude of between 3700 and 3970 m asl and has CRN ages that range from ~ 2 to 12 ka (includes 70 year, 2 ka, 3.2 ka, 4.4 ka, 11.7 ka ages). The t_1 terrace that onlaps this moraine at Milam is dated at ~ 7–8 ka (includes 5.0, 7.0, 7.8, and 8.0 ka ages). These ages indicate that the moraine has to be older than 7–8 ka.

Table 1
CRN ages calculated for samples in the Gori Ganga Valley

Sample #	Location	Landform	ID	Latitude (° ± 0.01°)	Longitude (° ± 0.01°)	Altitude (m)	Shielding factor factor ^a	¹⁰ Be ^b (10 ⁶ atoms/g)	Exposure age (ka) ^b	Exposure age with geomag. corr. ^c (ka)
R2	Rilkot	Fan	F ₂	30.31 N	80.21 E	3070	0.96	0.032 ± 0.002	0.92 ± 0.07	0.93 ± 0.07
R3	Rilkot	Fan	F ₂	30.31 N	80.21 E	3196	0.96	0.020 ± 0.002	0.54 ± 0.06	0.50 ± 0.06
R4	Rilkot	Fan	F ₂	30.31 N	80.21 E	3169	0.96	0.036 ± 0.004	0.98 ± 0.10	0.99 ± 0.10
R5	Rilkot	Terrace	T ₃	30.31 N	80.20 E	3351	0.96	0.169 ± 0.011	4.14 ± 0.26	4.69 ± 0.29
R6	Rilkot	Terrace	T ₃	30.31 N	80.20 E	3345	0.96	0.178 ± 0.007	4.38 ± 0.18	4.94 ± 0.20
R7	Rilkot	Terrace	T ₁	30.32 N	80.21 E	3163	0.96	0.046 ± 0.002	1.28 ± 0.06	1.34 ± 0.06
R8	Rilkot	Terrace	T ₁	30.32 N	80.21 E	3174	0.96	0.378 ± 0.009	10.35 ± 0.25	10.81 ± 0.26
R9	Rilkot	Terrace	T ₁	30.32 N	80.21 E	3161	0.96	0.667 ± 0.016	18.42 ± 0.44	19.31 ± 0.46
R10	Rilkot	Terrace	T ₁	30.32 N	80.21 E	3167	0.96	0.295 ± 0.007	8.11 ± 0.20	8.44 ± 0.21
R11	Rilkot	Terrace	T ₁	30.31 N	80.21 E	3149	0.96	0.238 ± 0.007	6.58 ± 0.19	6.99 ± 0.21
R12	Rilkot	Terrace	T ₁	30.31 N	80.21 E	3139	0.96	0.076 ± 0.003	2.10 ± 0.10	2.28 ± 0.10
R13	Rilkot	Terrace	T ₁	30.31 N	80.21 E	3136	0.96	0.034 ± 0.002	0.93 ± 0.07	0.95 ± 0.07
R14	Rilkot	Terrace	T ₁	30.31 N	80.21 E	3135	0.96	0.072 ± 0.004	1.99 ± 0.10	2.14 ± 0.11
R15	Rilkot	Terrace	T ₂	30.32 N	80.21 E	3262	0.98	0.163 ± 0.005	4.12 ± 0.13	4.66 ± 0.15
R18	Rilkot	Terrace	T ₂	30.32 N	80.21 E	3289	0.98	0.415 ± 0.019	10.35 ± 0.48	10.82 ± 0.51
R19	Bogdiar	Strath	–	30.21 N	80.23 E	2315	0.77	0.079 ± 0.004	4.55 ± 0.22	5.08 ± 0.24
R20	Bogdiar	Strath	–	30.20 N	80.23 E	2250	0.66	0.074 ± 0.004	5.19 ± 0.26	5.67 ± 0.28
R21	Lilam	Strath	–	30.12 N	80.25 E	1412	0.93	0.049 ± 0.003	4.26 ± 0.26	4.78 ± 0.29
NDL 2	Milam	Moraine	m ₄	30.45 N	80.12 E	3534	0.97	0.014 ± 0.005	0.31 ± 0.11	0.28 ± 0.10
NDL 4	Milam	Moraine	m ₄	30.45 N	80.12 E	3522	0.96	0.027 ± 0.004	0.61 ± 0.10	0.57 ± 0.09
NDL 9	Milam	Moraine	m ₃	30.45 N	80.13 E	3505	0.97	0.007 ± 0.005	0.16 ± 0.10	0.14 ± 0.09
NDL 10	Milam	Moraine	m ₃	30.45 N	80.13 E	3510	0.98	0.013 ± 0.002	0.28 ± 0.04	0.25 ± 0.04
NDL 15	Milam	Moraine	m ₂	30.46 N	80.13 E	3720	0.98	0.092 ± 0.013	1.81 ± 0.25	1.94 ± 0.27
NDL 16	Milam	Moraine	m ₂	30.45 N	80.13 E	3817	0.98	0.004 ± 0.002	0.08 ± 0.04	0.07 ± 0.04
NDL 18	Milam	Moraine	m ₁	30.45 N	80.13 E	4051	0.99	0.125 ± 0.005	2.03 ± 0.08	2.21 ± 0.08
NDL 19	Milam	Moraine	m ₁	30.45 N	80.13 E	4069	0.99	0.524 ± 0.015	8.45 ± 0.24	8.88 ± 0.26
NDL 20	Milam	Moraine	m ₁	30.45 N	80.13 E	4068	0.99	0.279 ± 0.007	4.50 ± 0.11	5.11 ± 0.13
NDL 21	Milam	Moraine	m ₁	30.45 N	80.13 E	4069	0.99	0.204 ± 0.007	3.29 ± 0.11	3.81 ± 0.12
NDL 22	Milam	Moraine	m ₁	30.45 N	80.13 E	4075	0.99	0.966 ± 0.024	15.56 ± 0.38	16.45 ± 0.40
NDL 23	Milam	Moraine	m ₂	30.45 N	80.14 E	3968	0.99	0.176 ± 0.006	2.99 ± 0.09	3.44 ± 0.11
NDL 24	Milam	Terrace	t ₁	30.43 N	80.16 E	3446	0.97	0.190 ± 0.065	4.38 ± 1.49	4.95 ± 1.68
NDL 25	Milam	Terrace	t ₁	30.43 N	80.16 E	3335	0.97	0.314 ± 0.014	7.67 ± 0.33	8.02 ± 0.35
NDL 26	Milam	Terrace	t ₁	30.43 N	80.16 E	3416	0.97	0.282 ± 0.016	6.59 ± 0.37	7.03 ± 0.40
NDL 27	Milam	Terrace	t ₁	30.43 N	80.16 E	3435	0.97	0.323 ± 0.008	7.48 ± 0.19	7.84 ± 0.20
NDL 29	Milam	Moraine	m ₂	30.43 N	80.16 E	3497	0.97	0.500 ± 0.015	11.17 ± 0.34	11.74 ± 0.36
NDL 30	Milam	Moraine	m ₂	30.43 N	80.16 E	3476	0.97	0.171 ± 0.005	3.87 ± 0.11	4.40 ± 0.13
NDL 32	Milam	Moraine	m ₂	30.41 N	80.16 E	3397	0.97	0.121 ± 0.005	2.85 ± 0.12	3.23 ± 0.14
NDL 44	Milam	Terrace	t ₃	30.43 N	80.15 E	3414	0.97	0.135 ± 0.031	3.16 ± 0.72	3.61 ± 0.82
NDL 45	Milam	Terrace	t ₃	30.43 N	80.15 E	3320	0.97	0.072 ± 0.004	1.78 ± 0.09	1.90 ± 0.10

No additional uncertainty was assigned arising from correction for geomagnetic field change. These ages were calculated with a sea level high latitude production of ¹⁰Be = 5.16 atoms/gram/quartz using the scaling factors of Lal (1991) as modified by Stone (2000).

^a The topographic shielding factor was determined using the methods of Nishiizumi et al. (1989).

^b Uncertainty includes only uncertainty in AMS measurement. Concentration is per gram quartz.

^c Corrected for time varying geomagnetic field as described in text. The uncertainty is carried over from that in the exposure age.

This disparity in ages may be the result of intense erosion of the moraine boulders. Alternatively, the terrace boulders may have inherited CRNs from a prior exposure and the t₁ terrace may actually be younger than the CRN ages indicate. However, the

similarity in age of three of the four terrace boulders makes it unlikely that the ages on the terrace are erroneously old. The most likely interpretation is that the moraine formed shortly before the terrace and is therefore early Holocene in age.

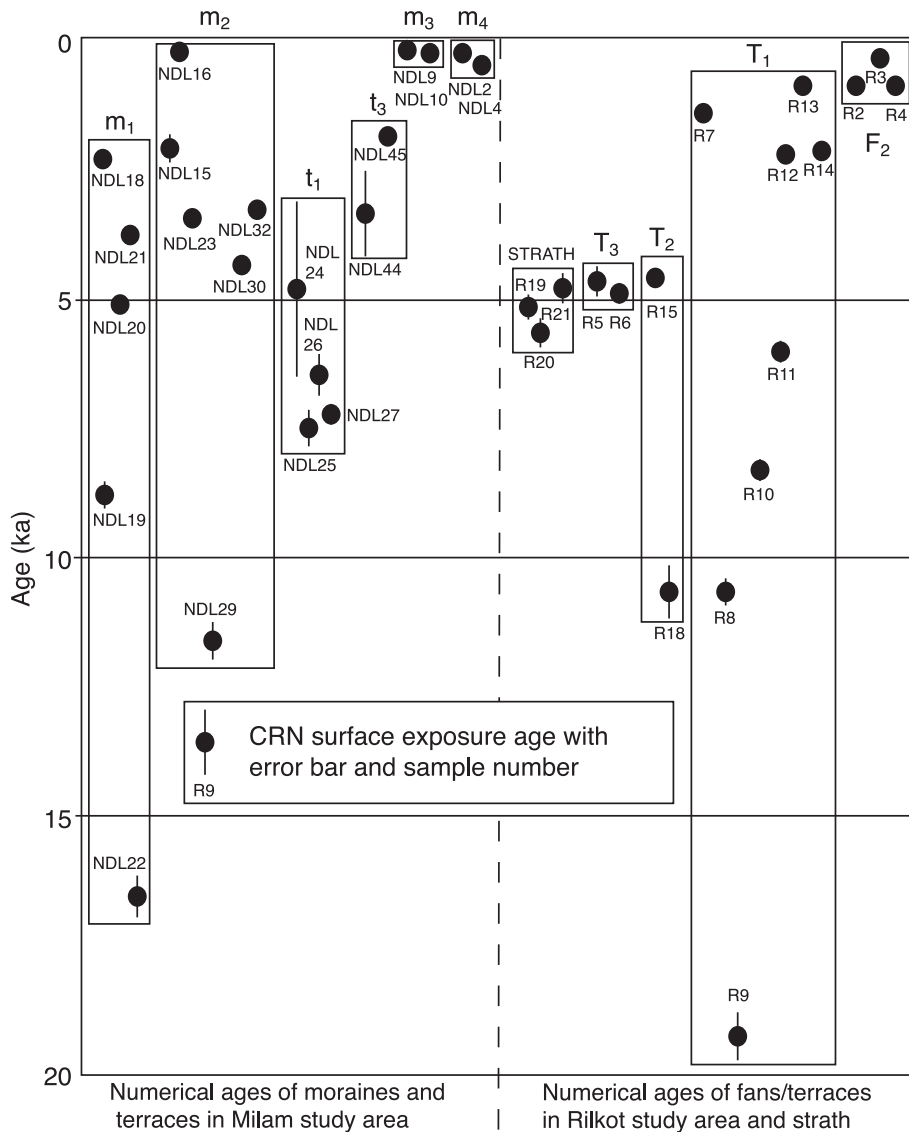


Fig. 16. CRN ages of moraines, fans, and terraces in the study area. Each box encloses the range of CRN ages calculated for each sample from the given landform. See Table 1 for detailed sample and landform ID information.

The oldest moraine dated has CRN ages that range between 2.2 and 16.5 ka (includes 2.2, 3.8, 5.1, 8.9, and 16.5 ka). Although only one dated boulder is Pleistocene in age, morphostratigraphically this moraine must pre-date the early Holocene moraine. We attribute the young CRN ages to intense weathering in this humid environment. The age of this moraine cannot be adequately defined by the CRN dating that

we have undertaken, but it is likely that it formed during the Late Pleistocene.

The origin of the diamictite ridge above Rilkot is problematic and could be interpreted as either glacial or mass movement deposits (cf. Benn and Owen, 2002; Fig. 1). However, we favor a glacial origin because the landform traverses the valley and is reminiscent of an end moraine, and it is broadly

coincident with a change in valley form from a typical broad U-shaped glaciated to deeply fluvial incised gorge to the south. If this deposit is tillite, then it marks the southern extent of glaciation in the Gori Ganga Valley and would possibly date to $\sim 4\text{--}5$ ka. However, the apparent degree of lithification of the diamictite and its streamlined denuded surface form suggests greater antiquity. The boulders that were dated using CRN from the surface of this landform might have been exhumed which would account for young ages. As such, they may not be dating the timing of the formation of the ridge but rather its reworking.

8. Fan succession

The fans and terraces in the Rilkot area formed during the Holocene, with CRN data suggesting deposition at $\sim 1\text{--}2$ and $4\text{--}5$ ka (Table 1; Fig. 16). The highest surfaces, T_2 and T_3 , which are morphostratigraphically similar, have a mean age of 4.8 ka ($n=3$, reject R18, age = 10.8 ± 0.5 ka). We believe this 4.8 ka age for this terrace is valid because (i) the three boulders used for the age calculation clearly had not moved since they were deposited; (ii) samples were collected from weathering resistant quartzites or quartz veins in schist; and (iii) boulders sampled were far removed from areas subject to rock falls. R18 was a deeply eroded schist on a lower portion of the ridge (Fig. 1) that might have been pre-exposed.

F_2 is dated to ~ 1 ka ($n=3$, samples R2–R4). Each of the boulders that were sampled was located toward the distal edge of the fan surface and exposed by at least 1 m, reducing the chances of rock fall or exhumation.

T_1 was sampled at two locations (Fig. 1, samples R7–R14). The results from each location varied widely (Table 1). This is likely due to the bedrock cliff located immediately to the west of this terrace and due to the strong potential for boulders to have been pre-exposed along the cliff face before tumbling down and coming to rest on the fan and terrace surfaces below. CRN data suggest that four of the eight samples dated from the surface of T_1 are derived boulders (R8–R11). This is based on their lithology (schists, identical to cliff lithology) and age (older than T_2 and T_3 that are situated ~ 100 m above this

depositional surface). The ages of the four samples that were not derived (R7, R12–R14) suggest that this terrace formed between ~ 1 and 2 ka, agreeing with the calculated age of F_2 that is morphostratigraphically equivalent to T_1 (Figs. 1 and 8B).

9. Discussion

Although glacial advances in Gori Ganga are poorly defined (Fig. 16), climatic inferences and correlation of moraine chronologies in the Nanda Devi region can be made with well-defined glacial chronologies in the Lahul and NW Garhwal Himalaya. In the Gangotri region of NW Garhwal, Barnard et al. (in press) suggested that glaciers are likely to have advanced during insolation maxima, citing glacial advances during the Late Glacial Interstadial, as well as at ~ 7 , 5, and 1 ka. The two oldest Gori Ganga moraines are in the Milam area and are Late Pleistocene/early Holocene in age. Although the widely scattered CRN ages broadly define the true age of these moraines, the tight clustering of ages at $\sim 7\text{--}8$ ka from a terrace that overlaps the younger of the two moraines sets a good lower limit on the age of moraine formation. We therefore suggest that these moraines formed sometime between the Late Glacial Interstadial and early Holocene advances that are found in the NW Garhwal Himalaya. In the Lahul Himalaya, Owen et al. (2001) showed that there was an extensive glacial advance (Batal Glacial Stage) during the Late Glacial Interstadial when the Chandra and Bhaga Valleys filled with ice. The oldest moraine in Gori Ganga might be coincident with the Batal Glacial Stage in Lahul. Owen et al. (2001) also showed evidence for a more limited glacial advance during the early Holocene, the Kulti Glacial Stage, when glaciers advanced <10 km from their present positions. The early Holocene moraines that we dated might correlate with the Kulti Glacial in Lahul. Historical records from Gangotri show small advances during the LIA and significant glacier retreat during the last several hundred years.

Barnard et al. (in press) built on the glacial and paraglacial work of Sharma and Owen (1996) and Owen and Sharma (1998) in the Gangotri region of NW Garhwal. These studies showed that fan and

terrace formation were intimately tied to glaciation and that sedimentation was rapid, consisted of reworked glacial deposits, and was coincident with glacial retreat. Furthermore, they showed that the timing of glacial advances was related to periods of increased insolation, when enhanced monsoon activity resulted in increased levels of snow accumulation at high altitudes resulting in positive glacier mass balance despite higher insolation. Similar connections between enhanced monsoon influence and glaciation have been recognized in the Hunza Valley of northern Pakistan and the Khumbu Himal of Nepal (Owen et al., 2002; Finkel et al., 2003). Benn and Owen (1998) suggested that glaciers throughout the Himalaya responded to a variety of climatic factors, including the influence of both the mid-latitude westerlies and the south Asian summer monsoon. Furthermore, they suggested that Himalayan glaciation might be asynchronous with Northern Hemisphere ice sheet growth and ocean cooling. These authors recognized minor advances associated with insolation maxima during the Late Glacial and early Holocene in the Himalaya (Sharma and Owen, 1996; Owen et al., 2001, 2002; Finkel et al., 2003; Barnard et al., in press). The fans in the Rilkot area of the Gori Ganga Valley formed during the mid- and late Holocene (i.e., 4–5 and 1–2 ka). Times of increased sedimentation during the mid-Holocene and Little Climatic Optimum were also recognized in NW Garhwal (Barnard et al., in press) and further support the hypothesis that glaciation occurs during periods of higher precipitation. The small LIA advance suggested in this study would correlate with the recognized Bhujbas advance in NW Garhwal (Sharma and Owen, 1996). At present, fans are starting to form that are related to the retreat of glaciers following the LIA.

The sedimentology of the fans in the Gori Ganga Valley are characteristic of reworked moraine material, containing striated, edge-rounded clasts in a sandy mud matrix (cf. Owen, 1994). Fan deposits are massive and thick (≥ 3 m), and no diamict sections contain evidence of more than two events. This suggests that paraglacial sedimentation occurred as high magnitude events that quickly and effectively redistributed glacial sediments. This agrees with the sedimentology described in fans from NW Garhwal Himalaya (Owen and Sharma, 1998; Barnard et al., in press).

The diamict units that were logged in the Gori Ganga Valley represent a history of rapid debris flow sedimentation separated by periods of slow aggradation, documented by numerous thin, sandy fluvial units with evidence of extensive bed form migration (i.e., cross-bedding). Based on the observation that contemporary fans have built out and blocked the Gori Ganga, the episodes of aggradation recorded in the sedimentary logs likely resulted from the river gradient decreasing when debris fans blocked the river during the Late Quaternary. Organic material in an F₂ fan section at Rilkot suggests a period of exposure long enough to allow for moderate soil development. Fan profile #3 (Fig. 10) represents a variety of low energy fluvial environments that accumulated over a large time span.

The average mid-Holocene to present bedrock incision rate was calculated to be 5.1 mm/year in the Gori Ganga Valley (Table 2). This rate is intermediate between rates calculated for the lower reaches of the Alaknanda Valley in central Garhwal by Barnard et al. (2001; 3.9 mm/year) and Vance et al. (2003; 2.7 mm/year) and the rates in the Gangotri region of NW Garhwal (ranging from 6.6 to 15.9 mm/year; Barnard et al., in press). Leland et al. (1998) documented an acceleration of average bedrock incision rates during the last 15 ka in Nanga Parbat and attributed this acceleration to an increase in discharge and/or sediment load related to deglaciation in the surrounding mountains following the major glacial advances of the Last Glacial. They also noted a substantial increase in incision rates during the last 7 ka, from 1–6 mm/year prior to 7 ka to 9–12 mm/year from 7 ka to the present. Vance et al. (2003) demonstrated that erosion rates correlate with relief. They calculated average denudation rates of 2.7 mm/year in the High Himalaya, 1.2 mm/year on the southern margin of the Tibetan Plateau, and 0.8 mm/year in the Lesser Himalaya. Therefore, the higher rates in Gangotri and the Gori Ganga Valley as compared to central Garhwal may be due to the greater relief, closer proximity to the eroding power of the glacial fronts (a few kilometers vs. tens of kilometers), weaker lithology (granite and gneiss vs. quartzite), and the time period represented (mid-Holocene vs. Late Pleistocene).

Strath terrace ages from the Gori Ganga Valley strongly correlate with the ~4–5 ka terrace ages

Table 2

Bedrock and fan incision rates calculated from CRN dating in the Gori Ganga Valley

Bedrock incision (strath)								
Landform ID #	Location	Alt (m)	¹⁰ Be exposure age (ka)	Height (m)	Incision rate (mm/year)			
R19	Bogdiar#1	2315	5.1 ± 0.2	26.0	5.1			
R20	Bogdiar#2	2250	5.7 ± 0.3	32.0	5.6			
R21	Lilam	1412	4.8 ± 0.3	22.0	4.6			
					Average = 5.1			
Fan and terrace incision								
Landform ID #	Location	Alt (m)	Approx. age of (ka)	Approx. age of lower terrace (ka)	Minimum thickness (m)	Minimum incision rate (mm/year)	Maximum thickness (m)	Maximum incision rate (mm/year)
T ₁	Rilkot	3140	1.0	0.0	19.0	19.0	19.0	19.0
T ₂	Rilkot	3301	4.7	0.0	195.0	41.5	195.0	41.5
T ₃	Rilkot	3357	4.8	1.0	183.0	48.2	217.0	57.1
F ₂	Rilkot	3123	1.0	0.0	34.0	34.0	34.0	34.0
						Average = 35.7		Average = 37.9

from the Rilkot area (Table 1). Strath terraces in the Gangotri region of NW Garhwal also formed during the mid-Holocene (ranging from 3.3 to 4.8 ka; Barnard et al., in press). This suggests that fluvial discharge and sediment loads were extremely high during this mid-Holocene period, possibly a result of deglaciation. Pratt et al. (2002) suggested that in central Nepal valleys were choked with sediment during the initial increase in monsoon precipitation at ~ 7 ka, and therefore strath terraces cannot be used to derive valley incision rates. However, the steep valley walls and the small strath terraces from which R19 and R20 were collected in the Gori Ganga Valley are extremely unlikely to have been sites of sediment storage (Fig. 15). No sedimentological evidence is available to suggest that there were any Late Quaternary episodes of extensive valley filling down stream of the Rilkot region where the fluvial system is contained within a narrow river gorge.

Rates of incision into the fans range between 19.0 and 57.1 mm/year (Table 2). This is relatively high compared to other Himalayan studies: for example, Watanabe et al. (1998) calculated denudation rates on debris cones in Langtang Himal that ranged between 3.2 and 15.6 mm/year, and Shroder et al. (1999) estimated denudation rates of 7 to 25 mm/year for localized glacier and river basins in the Nanga Parbat Himalaya. However, Shroder et al. (1999) also estimated rates as high as 120 mm/year that were asso-

ciated with catastrophic floods resulting from the breaking of repetitive landslide dams. High denudation rates in the Gori Ganga Valley could be a result of such flooding. A heightened monsoon during the last 4 ka in this part of the Himalaya, as suggested by Sharma and Gupta (1995) and Kotlia et al. (1997) and could also explain the high rates. Conversely, while denudation rates may be heightened during this period, high rates of erosion may have also produced erroneous ages by eroding boulder surfaces and/or exhuming boulders that were once buried and thus yielding artificially young ages. However, with few exceptions, boulders were selected that contained resistant lithologies (e.g., gneiss, quartzite) and significant relief (≥ 1 m) that would not have been affected by heightened erosion rates that persisted for the latter half of the Holocene. Furthermore, Riebe et al. (2001a,b) demonstrated that chemical weathering rates are largely independent of climate, suggesting that a heightened monsoon in NE Garhwal during the latter half of the Holocene would not have significantly eroded surface boulders. Therefore, the most likely scenario is that the Gori Ganga Valley is highly sensitive to climatic variations and that heightened monsoon activity resulted in very high denudation rates. Based on the young ages, determining if these high denudation rates continued in the Pleistocene or are an anomaly observed only in this one location for this time period is not possible. Certainly

these assertions are tentative and based on the limited data and should be tested by more work.

Sharma and Gupta (1995) conducted a vegetation study in Garhwal using radiocarbon dating that traced the regional climate back 1500 year. Their pollen analysis from a sedimentary profile in Nachiketa Tal (2550 m asl) indicates that a warm-humid climate dominated during the late Holocene. Kotlia et al. (1997) suggested dominantly wet conditions during the late Holocene based on one radiocarbon date ($3,700 \pm 100$ yr B.P.), and a concentration of humid pollen taxa and $^{13}\text{C}/^{12}\text{C}$ isotopic ratios of pollen extracted from a section in the Bhimtal-Naukuchiatal Lake basin in south-central Kumaun, SE of the study area. The high rates of erosion recognized in the Garhwal Himalaya during the mid- and late Holocene likely resulted from the dominantly humid conditions.

High uplift rates are undoubtedly a major factor in driving the background rates of denudation in the Himalaya. However, short-term rates range widely across the Himalaya; and therefore differences in landsliding, glacial influence, fluvial discharge, and sediment loads must also be considered when evaluating the factors that affect landscape evolution in different regions of the Himalaya. Each of these factors is, in turn, affected by climate. In NE Garhwal, a heightened monsoon during the last ~ 4 ka may explain the abnormally high rates of fan incision. Therefore, variations in the strength of the monsoon may be the most significant factor driving the short-term denudation of the Himalaya.

10. Conclusions

Sediment flux in the Gori Ganga Valley has been extremely high during the Late Quaternary. Our CRN dates broadly define the moraine ages to the Late Glacial Interstadial, early Holocene, late Holocene, and LIA. No moraines predate the Late Pleistocene. The fans are Holocene in age, with CRN ages clustering between 1 and 2, 4 and 5, and 7 and 8 ka. This is similar to ages for fans in NW Garhwal. The fans comprise bouldery diamicts, with derived clasts of glacial origin. The sedimentology, geomorphology, and the broad coincidence of moraine and fan ages support the view that fans are paraglacial in origin. Sediment denudation rates for the Holocene are high,

ranging from ~ 19 to 57 mm/year. This supports the hypothesis that the monsoon is a powerful influence on short-term rates of landscape evolution in the Garhwal Himalaya. In contrast, bedrock incision rates for the Gori Ganga Valley are ~ 5 mm/year. Although sediments are more easily eroded than bedrock, the high fan incision rates help demonstrate the importance of paraglaciation for landscape evolution in the Himalaya. This research, therefore, demonstrates that despite climatic variations, the long-term valley incision is relatively constant across the mountain range, but climatic oscillation helps drive major landscape changes. As such, the monsoon is a powerful factor in enhancing denudation and sediment transfer rates in this part of the Himalaya, and thus depositional landforms do not survive more than a few thousand years.

Acknowledgements

Funding for the field component of this project was provided by a grant from the University Research Expeditions Program (UREP). Many thanks to the UREP volunteers for their financial and field support, particularly to Patrick Smith for his assistance with the geomorphic mapping. The cosmogenic radionuclide dating analysis was undertaken at the Lawrence Livermore National Laboratory (under DOE contract W-7405-ENG-48) as part of an IGPP/LLNL research grant and a Student Employee Graduate Research Fellowship.

References

- Barnard, P.L., Owen, L.A., Sharma, M.C., Finkel, R.C., 2001. Natural and human-induced landsliding in the Garhwal Himalaya of northern India. *Geomorphology* 40, 21–35.
- Barnard, P.L., Owen, L.A., Finkel, R.C., in press. Style and timing of glacial and paraglacial sedimentation in a monsoonal-influenced high Himalayan environment, the upper Bhagirathi Valley, Garhwal Himalaya. *Special Issue of Sedimentary Geology*, Elsevier. 20 pp.
- Benn, D.I., Evans, D.J., 1998. *Glaciers and Glaciation*. Arnold, London. 734 pp.
- Benn, D.I., Owen, L.A., 1998. The role of the Indian summer monsoon and the mid-latitude westerlies in Himalayan glaciation: review and speculative discussion. *Journal of the Geological Society* 155, 353–363.

- Benn, D.I., Owen, L.A., 2002. Himalayan glacial sedimentary environments: a framework for reconstructing and dating former glacial extents in high mountain regions. *Quaternary International* 97–98, 3–25.
- Bojar, A.V., Bregar, M., Fritz, H., 2001. Structural evolution and cooling of the high Himalayan crystalline in the Gori Ganga Valley, Kumaon, India. *Journal of Asian Earth Sciences* 19 (3A), 5–6.
- Davis, J.C., Proctor, I.D., Southon, J.R., Caffee, M.W., Heikkinen, D.W., Roberts, M.L., Moore, T.L., Turteltaub, K.W., Nelson, D.E., Loyd, D.H., Vogel, J.S., 1990. LLNL/UC AMS facility and research program. *Nuclear Instruments & Methods in Physics Research B52*, 269–272.
- Eyles, N., Dearman, W.R., Douglas, T.D., 1983. The distribution of glacial landforms in Britain and North America. In: Eyles, N. *Glacial Geology*. Pergamon, Oxford, UK, pp. 213–228.
- Finkel, R.C., Owen, L.A., Barnard, P.L., Caffee, M.W., 2003. Beryllium-10 dating of Mount Everest moraines indicates a strong monsoonal influence and glacial synchronicity throughout the Himalaya. *Geology* 31, 561–564.
- Heim, A., Gansser, A., 1975. *Central Himalaya Geological Observations of the Swiss Expedition 1936*. Hindustan Publishing, Delhi.
- Indian Meteorological Department, 1989. *Climate of Uttar Pradesh*. Government of India Publication, New Delhi, pp. 372–375.
- Janapangi, B.S., 1975. A note on the observations made on some glaciers of Malla Johar in 1966. *Records of the Geological Survey of India* 2, 240–247.
- Kohl, C.P., Nishiizumi, K., 1992. Chemical isolation of quartz for measurement of in situ-produced cosmogenic nuclides. *Geochimica et Cosmochimica Acta* 56, 3583–3587.
- Kotlia, B.S., Bhalla, M.S., Sharma, C., Rajagopalan, G., Ramesh, R., Chauhan, M.S., Mathur, P.D., Bhandari, S., Chacko, S.T., 1997. Palaeoclimatic conditions in the upper Pleistocene and Holocene Bhimtal-Naukuchiatal Lake basin in the south-central Kumaun, north India. *Palaeogeography, Palaeoclimatology, Palaeoecology* 130, 307–322.
- Kumar, G., Hyderi Mehdi, S., Prakash, G., 1975. Observations on some glaciers of Kumaon Himalaya, U.P. *Records of the Geological Survey of India* 2, 231–239.
- Lal, D., 1991. Cosmic ray labelling of erosion surfaces: in situ nuclide production rates and erosion rates. *Earth and Planetary Science Letters* 104, 424–439.
- Leland, J., Reid, M.R., Burbank, D.W., Finkel, R., Caffee, M., 1998. Incision and differential bedrock uplift along the Indus River near Nanga Parbat, Pakistan Himalaya, from ^{10}Be and ^{26}Al exposure age dating of straths. *Earth and Planetary Science Letters* 154, 93–107.
- Nishiizumi, K., Winterer, E.L., Kohl, C.P., Lal, D., Arnold, J.R., Klein, J., Middleton, R., 1989. Cosmic ray production rates of ^{10}Be and ^{26}Al in quartz from glacially polished rocks. *Journal of Geophysical Research* 94, 17907–17915.
- Owen, L.A., 1989. Terraces, uplift and climate in the Karakoram Mountains, northern Pakistan: Karakoram intermontane base and evolution. *Zeitschrift für Geomorphologie* 76, 117–146.
- Owen, L.A., 1994. Glacial and non-glacial diamictites in the Karakoram Mountains and western Himalayas. In: Warren, W.P. *Formation and Deformation of Glacial Deposits*. Balkema, Rotterdam, pp. 9–28.
- Owen, L.A., Sharma, M.C., 1998. Rates of paraglacial fan formation in the Garhwal Himalaya: implications for landscape evolution. *Geomorphology* 26, 171–184.
- Owen, L.A., Benn, D.I., Derbyshire, E., Evans, D.J., Mitchell, W.A., Thompson, D., Richardson, S., Lloyd, M., Holden, C., 1995. The geomorphology and landscape evolution of the Lahul Himalaya, northern India. *Zeitschrift für Geomorphologie* 39, 145–174.
- Owen, L.A., Sharma, M.C., Bigwood, R., 1996. Landscape modification and geomorphological consequences of the 20th October 1991 earthquake and the July–August 1992 monsoon in the Garhwal Himalaya. *Zeitschrift für Geomorphologie* 103, 359–372.
- Owen, L.A., Gualtieri, L., Finkel, R.C., Caffee, M.W., Benn, D.I., Sharma, M.C., 2001. Cosmogenic radionuclide dating of glacial landforms in the Lahul Himalaya, northern India: defining the timing of Late Quaternary glaciation. *Journal of Quaternary Science* 6, 555–563.
- Owen, L.A., Finkel, R.C., Caffee, M.W., Gualtieri, L., 2002. Timing of multiple glaciations during the Late Quaternary in the Hunza Valley, Karakoram Mountains, northern Pakistan: defined by cosmogenic radionuclide dating of moraines. *Geological Society of America Bulletin* 114 (5), 593–604.
- Paul, S.K., 1998. Geology and tectonics of the central crystallines of northeastern Kumaon Himalayas, India. *Journal of Nepal Geological Society* 18, 151–167.
- Paul, S.K., Bartarya, S.K., Rautela, P., Mahajan, A.K., 2000. Catastrophic mass movement of 1998 monsoons at Malpa in Kali Valley, Kumaun Himalaya (India). *Geomorphology* 25, 169–180.
- Pratt, B., Burbank, D.W., Heimsath, A., Ojha, T., 2002. Impulsive alluviation during early Holocene strengthened monsoons, central Nepal Himalaya. *Geology* 30 (10), 911–914.
- Riebe, C.S., Kirchner, J.W., Granger, D.E., Finkel, R.C., 2001a. Minimal climate control on erosion rates in the Sierra Nevada, California. *Geology* 29 (5), 447–450.
- Riebe, C.S., Kirchner, J.W., Granger, D.E., Finkel, R.C., 2001b. Strong tectonic and weak climate control of long-term chemical weathering rates. *Geology* 29 (6), 511–514.
- Sharma, C., Gupta, A., 1995. Vegetational history of Nachiketa Tal, Garhwal Himalaya, India. *Journal of Nepal Geological Society* 10, 29–34.
- Sharma, M.C., Owen, L.A., 1996. Quaternary glacial history of the Garhwal Himalaya, India. *Quaternary Science Reviews* 15, 335–365.
- Shroder, J.F., Scheppy, R.A., Bishop, M.P., 1999. Denudation of small alpine basins, Nanga Parbat Himalaya, Pakistanin Khan. *Arctic, Antarctic, and Alpine Research* 31 (2), 121–127.
- Stone, J.O., 2000. Air pressure and cosmogenic isotope production. *Journal of Geophysical Research* 105, 23753–23759.
- Valdiya, K.S., 1980. *Geology of Kumaon Lesser Himalaya*. Wadia Institute of Himalayan Geology, Dehra Dun, India. 299 pp.

- Vance, D., Bickle, M., Ivy-Ochs, S., Kubik, P.W., 2003. Erosion and exhumation in the Himalaya from cosmogenic isotope inventories of river sediments. *Earth and Planetary Science Letters* 206, 273–288.
- Watanabe, T., Dali, L., Shiraiwa, T., 1998. Slope denudation and the supply of debris to cones in Langtang Himal, central Nepal Himalaya. *Geomorphology* 26, 185–197.
- Weidinger, J.T., 1998. Case history and hazard analysis of two lake-damming landslides in the Himalayas. *Journal of Asian Earth Sciences* 16, 323–331.